Journal of Applied Electrochemistry **32**: 687–692, 2002.

Advanced Sn/C composite anodes for lithium ion batteries

Y. LIU[1]*, J.Y. XIE[1], Y. TAKEDA[2] and J. YANG[1]
[1]*Energy Science and Technology Laboratory, Shanghai Institute of Metallurgy, Chinese Academy of Sciences, Shanghai 200050, China*
[2]*Department of Chemistry, Mie University, Tsu, Mie 514-8507, Japan*
*(*author for correspondence, fax: +86 21 32200534, e-mail: liuyu@mail.sim.ac.cn)*

Received 20 June 2001; accepted in revised form 19 February 2002

Key words: carbonaceous mesophase spherules, lithium ion battery, organic tin salt, porous carbon, Sn/C composite anode

Abstract

Metallic tin was deposited in fine particulate form on the surface of carbonaceous mesophase spherules (CMS) and in the pores of porous carbon by the decomposition and reduction of tin(II) 2-ethylhexanoate at 450 °C. The Sn/C composite powders obtained were used as anode materials for lithium ion cells. Electrochemical cycling tests of coin cells show that the dispersion of tin into the carbonaceous materials enhances the reversible capacity of the electrodes. The capacity retention at the 50th cycle is 91% for Sn/CMS composite containing 22% tin, against 428 mAh g^{-1} at the first cycle. With further increase in tin content, the capacity fade upon cycling is more rapid.

1. Introduction

Graphic materials have been widely used as intercalation anodes in rechargeable lithium batteries. In general, they have high initial efficiency and excellent capacity retention on cycling. However, their reversible capacities are limited to below 370 mAh g^{-1}, much lower than those of some lithium alloys [1]. For example, the theoretical capacity of $Li_{22}Sn_5$ is about 990 mAh g^{-1}. A major problem related to lithium alloy as anode materials is the mechanical and cycling instability caused by the drastic volume changes during lithium insertion and extraction [2, 3]. This is especially serious under high lithium utilization. Although tin-based composite oxides demonstrated reversible capacity of more than 550 mAh g^{-1} and good cycling stability [4], the high initial irreversibility related to the conversion of tin oxide into metallic tin and Li_2O limits its practical application. In addition, a further study revealed that aggregation of tin in the oxides could not be avoided over cycling, which led to volume mismatch and subsequent capacity fade [5, 6].

To obtain new anode materials with improved cycle performance, much recent study has focused on composites of lithium storage metals and carbonaceous materials. Pyrolyzed polysiloxanes [7, 8], highly dispersed silver on carbon [9] and nano-SnSb/carbon composite [10] are representatives of this class of anode material. The composite electrodes generally provide a higher capacity than graphite and a better cycling stability than the respective metallic host. The improved cyclability is attributed to the small volume expansion of carbon for lithium accommodation (about 9% for graphite). Furthermore, it is expected that soft and ductile carbon could endure the volume change of the metallic host and reduce the mechanical stress within the electrode, and thereby prevent disintegration. However, most of the metal/carbon composites are still inferior to carbonaceous materials in cyclability, especially if a metallic host with high insertion capacity is used as a component. It seems that to a great extent the cycle performance of composite systems depends on the distribution of the metallic host and the contact strength between the two active materials. It was reported that the Sn-KS6 composite, prepared by chemically reductive precipitation in aqueous solution, still suffered from noticeable capacity fade over cycling [11]. In this work metallic tin is deposited on the surface of carbon, and inside porous carbon, by the reduction of organic tin salt at high temperature. This preparation method is suitable for mass production in industry. The electrochemical cycling behaviour of the Sn/C composite materials is investigated via coin cells.

2. Experimental details

2.1. *Material preparation*

Carbonaceous mesophase spherules (CMS) named G16 (BET surface area: 1.92 m^2 g^{-1}, typical particle size: 15 μm) and porous carbon (PC) named HSAG100 (BET

surface area 100 $m^2\ g^{-1}$, average particle size: 26 μm) were used as matrices for tin deposition. These carbon materials are commercially available. Tin(II) 2-ethylhexanoate was from Aldrich. Its tin content was 29.4 wt %.

The basic procedures for preparing tin/carbon composites were as the follows. CMS powder was suspended in a solution containing tin(II) 2-ethylhexanoate and tetrahydrofuran (THF) solvent. The slurry obtained was stirred and slightly heated to remove bubbles in solution and to evaporate THF solvent until it became quite viscous. Then the THF was further removed in an oven at 80 °C. The THF-free mixture was transferred into a quartz reaction tube. After mixed gas containing 4.9% H_2 and 95.1% Ar passed the tube for 20 min, the tube was moved into preheated furnace at 450 °C under the protection of the mixed gas. The reaction temperature of 450 °C was maintained for 20 min and the quartz tube was then quickly withdrawn from the furnace and quenched to room temperature. For preparing Sn/PC composite material, an ultrasonic treatment was adopted for slurry containing porous carbon, tin(II) 2-ethylhexanoate and THF to allow the tin salt to penetrate into the pores of the carbon. The following steps were the same as described above.

For comparison, fine tin powder (typical particle size <0.8 μm) was prepared by chemical precipitation [12].

2.2. *Electrode fabrication*

A given weight of Sn/C composite (or Sn, C) powder and acetylene black were added into polyvinlidene fluoride (PVdF)/l-methyl-2-pyrrolidone solution and stirred to form a slurry, which was then coated onto 20 μm thick copper foil. After solvent evaporation, the film obtained was cut into disc-form electrode (dia. 14 mm) and further dried at 130 °C under vacuum for 2 h. Finally, CMS-based electrodes were compacted at 3 MPa and PC-based ones at 1 MPa. The mass of an electrode was about 4 mg cm^{-2}. All the electrodes contained 4% acetylene black, 8% PVdF and 88% active material (wt %).

2.3. *Electrochemical and XRD measurements*

Discharge (i.e., lithium insertion) and charge (i.e., lithium extraction) performance of the electrodes was evaluated via coin cells (typed 2025) containing 1 M $LiPF_6$/ethylene carbonate plus diethyl carbonate (1:1, vol.) from the Mitsubishi Chemical Company. The cells were assembled in a glove box using a lithium counter electrode and a microporous polypropylene separator. Unless stated otherwise, cycling tests were carried out under a controlled cut-off voltage between 0 and 1.5 V and at a constant current density of 0.2 mA cm^{-2}. The rest time between charge and discharge was 1 min.

The structure change of the composite electrodes during cycling was followed by powder X-ray pattern measurements using automated powder diffractometer with CuK_α radiation. After the cycling test, lithium was further removed from the electrodes at 0.05 mA cm^{-2} until 2 V vs Li.

3. Results and discussion

3.1. *Sn/CMS composite electrodes*

Carbonaceous mesophase spherules (CMS) and mesocarbon microbead (MCMB) have been widely used as anode materials in commercial rechargeable lithium batteries. In view of the possibility of practical application, CMS was firstly chosen as matrix for tin deposition. Figure 1 illustrates a SEM photograph of Sn/CMS composite powder containing 22% tin. Reduced metallic tin is finely dispersed and deposited on the CMS particle surface. The typical tin particle size is below 0.5 μm. By decomposition of the multicarbon organic tin salt, part of the carbon may also be deposited together with tin and encircle the tin particles. This may enhance the connecting strength between the tin and the carbon matrix. In addition, the distance between two tin particles is sufficient to prevent particle contact after volume expansion. Such a configuration seems able to reduce the mechanical stress caused by the volume effect and improve the morphological and conducting stability of the composite. The first discharge and charge profile of the obtained Sn/CMS composite, in comparison with pure CMS and tin, is shown in Figure 2. The composite electrode has an obvious discharge and charge character of pure CMS and pure tin. However, it can be noted that lithium insertion into the tin host in the composite electrode corresponds to a higher voltage polarization (voltage plateau: ~0.32 V, against 0.43 V for the tin electrode). This phenomenon is understandable, since dispersed tin in the composite electrode has a far smaller contact area with electrolyte than the pure tin electrode.

The cycling behaviour of the electrodes containing different tin contents was examined. Table 1 lists the first cycle data for these electrodes. With increasing tin

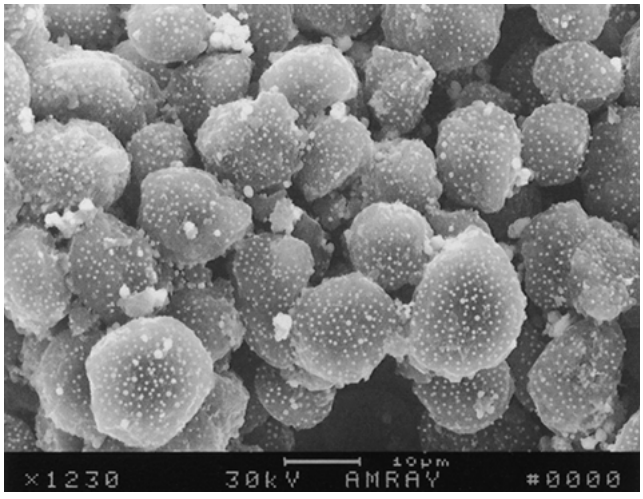

Fig. 1. SEM image of Sn/CMS composite powder containing 22% tin.

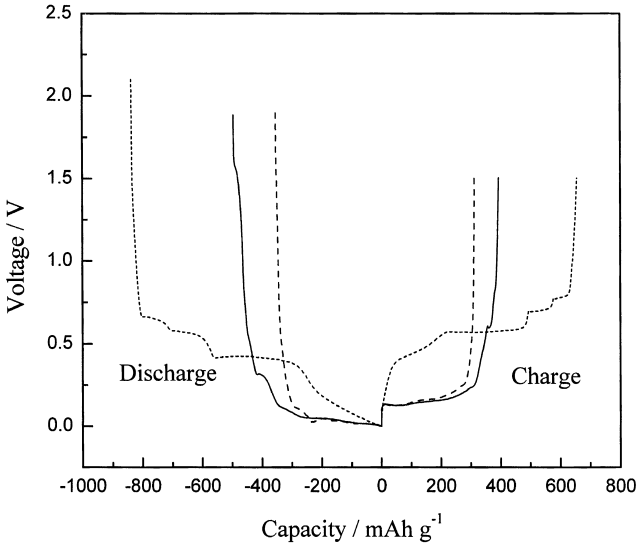

Fig. 2. First cycle profiles for CMS, tin and their composite with 22% tin. Key: (——) Sn/CMS compostite; (– – –) CMS; (- - -) Sn.

Table 1. The first cycle data for Sn/CMS composite electrodes with different tin contents

Tin content/wt %	0	13	22	31	58	100
Discharge capacity/mAh g^{-1}	353	427	534	591	739	838
Charge capacity/mAh g^{-1}	314	359	428	465	556	655
Coulombic efficiency/%	89	84	80	79	75	78

content, the reversible capacity rises, but the coulombic efficiency drops. If the reversible capacity of CMS in the composite electrodes is regarded as the same as that of the pure CMS electrode, the tin in the electrodes can deliver a reversible capacity of about 800 mAh g^{-1}. This value is higher than the 645 mAh g^{-1} of a pure tin electrode. Figure 3 exhibits the cycling behavior of the different electrodes. The capacity fade on cycling is rapid at a high tin content. SEM measurements reveal that tin particles larger than 2 μm apparently increase in the composite powder containing 58% tin and the particle distribution is not so uniform as that in a powder with low tin content. Such composite will face a nonuniform volume change for lithium insertion and extraction. Moreover, subdivision of the big tin particles and their detachment from carbon may take place during cycling. As a result, the conducting and cycling performance of the electrode is degraded. With decreasing tin content, its cyclability becomes comparable with that of CMS. Taking account of both capacity and cyclability, 22% tin content is suitable. The electrode provides a reversible capacity of about 395 mAh g^{-1} and the capacity retention at the 50th cycle is 91%, against 428 mAh g^{-1} at the first cycle. After the first cycle, its cycle efficiency rises rapidly and closes to that of the CMS electrode (Figure 4). In contrast, the efficiency of the tin electrode is smaller at the second and third cycle. Gradual electronic isolation of Li–Sn alloy material arising from the strong volume change is responsible for this.

Figure 5 shows the effect of current density on the discharge and charge characteristics at the 30th cycle. As the current density is enhanced from 0.1 to 0.8 mA cm^{-2}, the capacity loss is only about 5% and parts of the discharge and charge curves remain overlapping. This suggests that the electrode system has fast electrochemical kinetics and can be applied in a relatively wide range of current density.

The structure change of the composite electrode during cycling was investigated by XRD measurements. Figure 6 shows XRD patterns of a Sn/CMS composite electrode containing 22% tin. Layered graphite in CMS and β-Sn are reactant phases in the electrode. After the 30th cycle, the tin peak intensity becomes much weaker

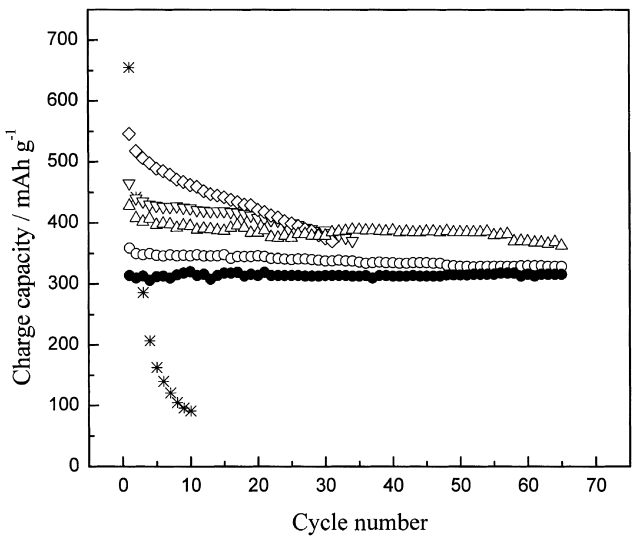

Fig. 3. Cycling performance of CMS, tin and Sn/CMS composites. Key: (✳) 100% Sn; (◇) 58% Sn; (▽) 31% Sn; (△) 22% Sn; (○) 13% Sn; (●) 0% Sn.

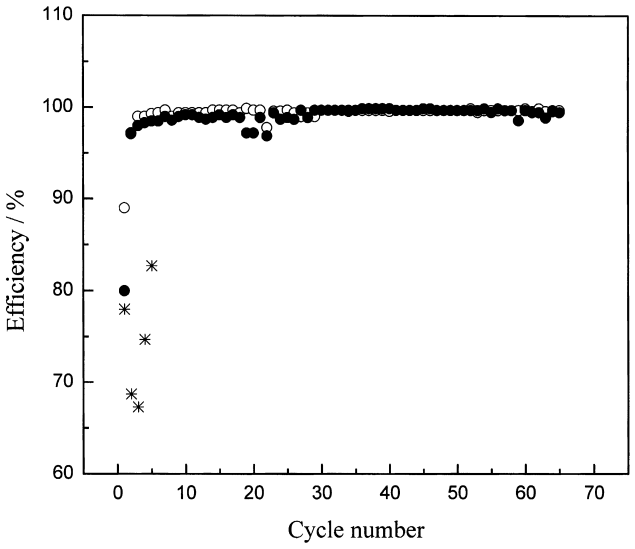

Fig. 4. Coulombic efficiency of CMS, tin and the composite containing 22% tin during cycling. Key: (○) CMS; (✳) Sn; (●) Sn/CMS composite.

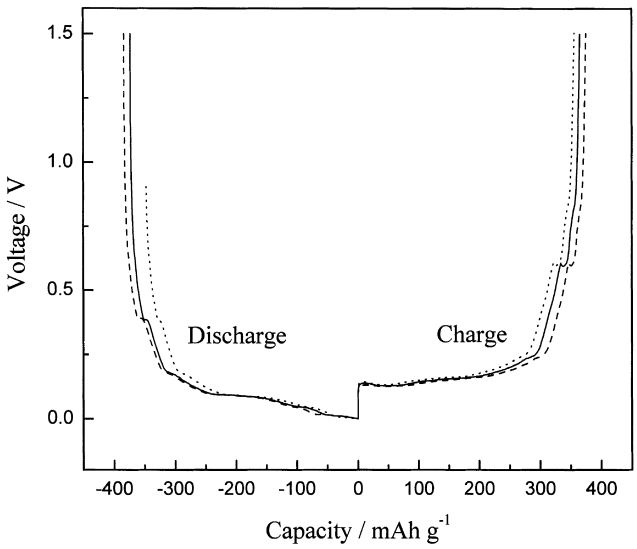

Fig. 5. Discharge and charge profiles at the 30th cycle for the composite electrode containing 22% tin. Current density: (– – – –) 0.1, (——) 0.6 and (- - - - -) 0.8 mA cm^{-2}.

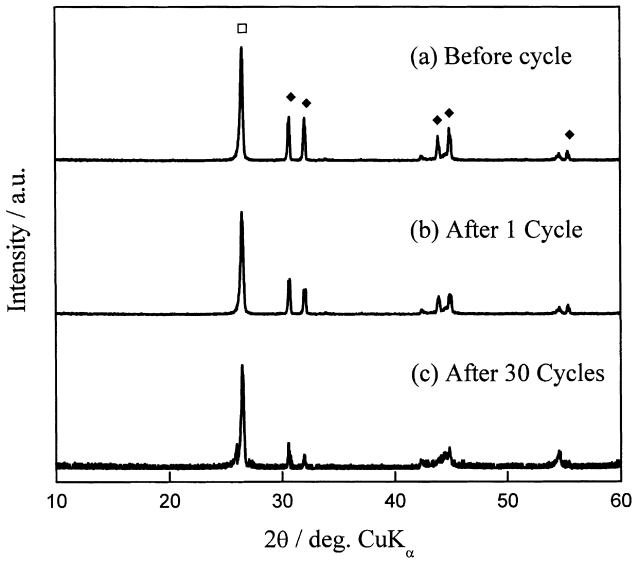

Fig. 6. XRD patterns of the composite electrode with 22% tin before and after cycling test. Key: (♦) β-Sn; (□) CMS.

than that after the first cycle, indicating that continuous lithium insertion and extraction to 100% extent leads to a subdivision of the tin particles and deterioration of the crystalline structure of metallic tin. However, the gradual pulverization of the tin host does not result in significant capacity loss. The electrode maintains a higher capacity than carbon from beginning to end. This means that a low-crystalline (or even amorphous) tin host in this electrode system still retains some lithium accommodation capability.

3.2. *Tin/porous carbon composite electrodes*

A further possibility is to disperse metallic tin into porous carbon. As described in the experimental part,

Table 2. The first cycle data for Sn/PC composite electrodes with different tin contents

Tin content/wt %	0	12	38	75	100
Discharge capacity/mAh g^{-1}	559	647	716	908	838
Charge capacity/mAh g^{-1}	241	304	380	563	655
Coulombic efficiency/%	43	47	53	62	78

such a composite material was prepared by using a dilute tin salt solution and permeating the solution into the carbon pores via ultrasound, followed by drying and heat treatment. We assumed that the soft and flexible carbon matrix could tolerate the volume change of embedded tin host and support the dispersed tin better. Table 2 lists the first cycle data for this type of composite material, in comparison with porous carbon and tin. The first discharge capacity of porous carbon is extremely high, but its coulombic efficiency is only 44%. The low faradaic yield can be attributed to electrolyte decomposition and subsequent surface filming. The large specific surface area of the porous carbon (100 m^2 g^{-1}) consumes a lot of charge for the filming process and thereby it causes a large irreversible capacity at the first cycle. Since pure tin has a far better initial reversibility than porous carbon, an increase in the tin content in the Sn/PC composite enhances the first cycle efficiency.

Figure 7 exhibits the first cycle profiles for porous carbon and Sn/PC composite containing 38% tin. Differing from CMS-based electrodes, lithium insertion into PC-based electrodes produces a voltage plateau near 0.7 V. This is linked to electrolyte decomposition as described above. In the charging process, the voltage change trend of the composite electrode can be clearly divided into two parts. Lithium is mainly extracted from carbon below 0.25 V and from tin host at a higher

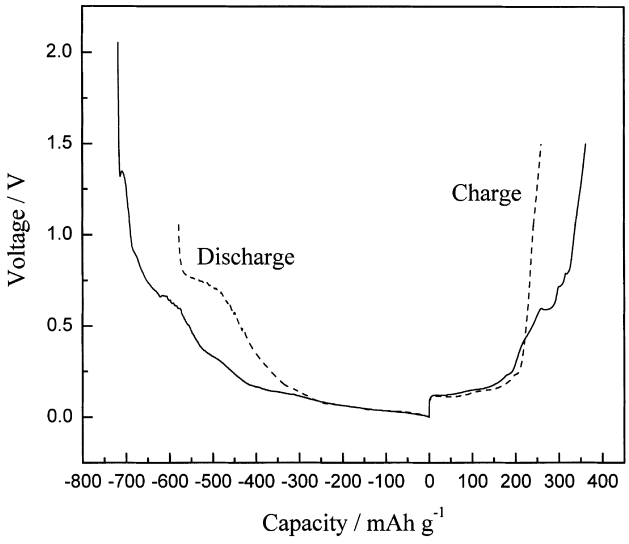

Fig. 7. First cycle profiles for porous carbon and a composite containing 38% tin. Key: (——) Sn/PC composite; (– – – –) porous carbon.

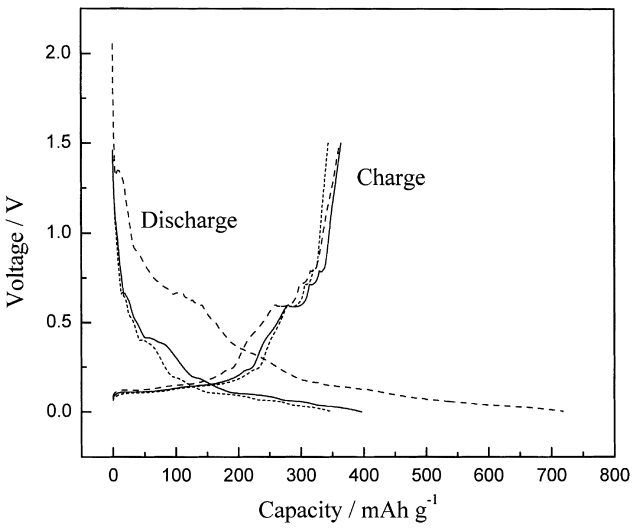

Fig. 8. Discharge and charge profiles for the composite electrode containing 38% tin. Key: (– – – –) cycle 1; (——) cycle 2; (- - - -) cycle 30.

voltage. Figure 8 further shows the discharge and charge curves for the composite electrode. At the second cycle, the irreversible voltage plateaux disappear and the electrode reflects the more distinct discharge and charge characteristics of metallic tin. The plateau lengths related to alloying and dealloying are apparently shortened after the 30th cycle and the cycle capacity is correspondingly reduced. The result appears to be caused by deterioration of the tin host as demonstrated in Figure 5.

It is observed from Figure 9 that a further increase in the tin content in porous carbon leads to rapid capacity loss on cycling. The key influencing factor here may not be the change in the tin microstructure, but the deteriorating mechanical and conducting performance of the electrode. At least two problems are difficult to solve by the preparation method of the Sn/PC composite described in this study: (i) part of the tin is deposited on the outer surface of the porous carbon. SEM measurement shows that the exposed tin particles become larger and the distribution uniformity is poorer with enhanced tin content; (ii) tin deposited in the carbon pores occupies only a small part of the space, so that the carbon may not lock the embedded tin well, even after the tin volume expansion. On the other hand, the depth of the tin salt solution permeation in the carbon particles and how much tin is embedded in the carbon pores are still unclear at this stage. Although the deposition of a small amount of tin slightly increases the cycle capacity and maintains a good cycling stability, the initial efficiency and the total capacity remain low. From this point of view, the Sn/CMS composite has an obvious advantage over Sn/PC as anode material for lithium ion batteries.

4. Conclusions

Decomposition and reduction of tin(II) 2-ethylhexanoate at 450 °C provides a simple but effective preparation method for Sn/C composite materials. Although the reaction temperature is higher than the melting point of tin (232 °C), tin can be finely and uniformly deposited on the carbon surface with controlled reaction time and tin content. The composite material delivers a larger reversible capacity than the respective carbon matrix, and the Sn/CMS composite is superior to the Sn/porous carbon composite in terms of cycle efficiency and capacity. The cyclability is, to a great extent, dependent on the tin content in the composites. The capacity loss of the Sn/CMS composite containing 22% tin is about 9% at the 50th cycle. The deterioration of the crystalline structure of the tin may be a major reason for the capacity fade at low tin contents. The poor capacity retention at high tin content (>30%) can be mainly

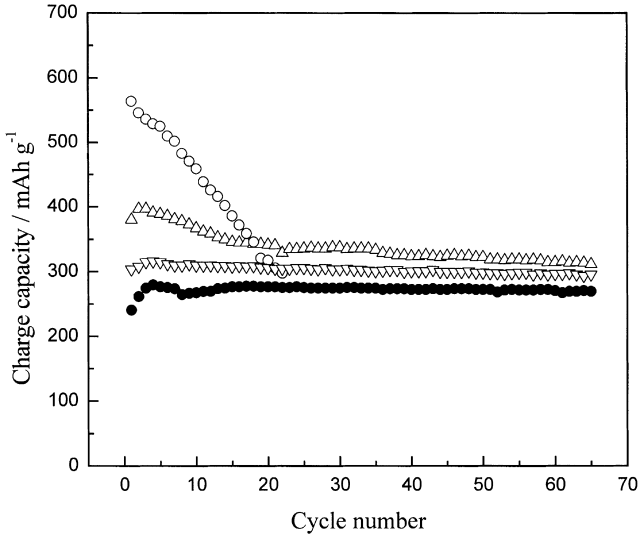

Fig. 9. Cycling performance of porous carbon and Sn/PC composites. Key: (●) 0% Sn; (▽) 12% Sn; (△) 38% Sn; (○) 75% Sn.

attributed to mechanical and conducting deterioration of the electrode arising from the severe volume change.

References

1. J.O. Besenhard, J. Yang and M. Winter, *J. Power Sources* **68** (1997) 87.
2. D. Fauteux and R. Koksbang, *J. Appl. Electrochem.* **23** (1993) 1.
3. W.C. Maskell and J.R. Owen, *J. Electrochem. Soc.* **132** (1985) 1602.
4. Y. Idota, T. Kubota, A. Matsufuji, Y. Maekawa and T. Miyasaka, *Science* **276** (1997) 1395.
5. Ian A. Courtney and J.R. Dahn, *J. Electrochem. Soc.* **144** (1997) 2943.
6. T. Brousse, R. Retoux and D.M. Schleich, The 39th Battery Symposium in Japan, 25–27 Nov., 1998, Seidai, Japan, Extended Abstract, p. 407.
7. A.M. Wilson and J.R. Dahn, *J. Electrochem. Soc.* **142** (1995) 326.
8. W.B. Xing, A.M. Wilson, K. Eguchi, G. Zank and J.R. Dahn, *J. Electrochem. Soc.* **144** (1997) 2410.
9. J. Aragane, K. Matsui, H. Andoh, S. Suzuki, H. Fukuda, H. Ikeya, K. Kitaba and R. Ishikawa, *J. Power Sources* **68** (1997) 13.
10. L.H. Shi, H. Li, W. Lu, X.J. Huang and L.Q. Chen, Proceedings of the 7th Asian Conference on Solid State Ionics, Fuzhou, China, 29 Oct.–4 Nov. 2000, pp. 357–340.
11. J.Y. Lee, R.F. Zhang and Z.L. Liu, *J. Power Sources* **90** (2000) 70.
12. J. Yang, M. Wachtler, M. Winter and J.O. Besenhard, *Electrochem. Solid State Lett.* **2** (1999) 161.